Colloids and Surfaces B: Biointerfaces 168 (2018) 94–102

Contents lists available at ScienceDirect

Colloids and Surfaces B: Biointerfaces

journal homepage: www.elsevier.com/locate/colsurfb

Adsorption of polysorbate 20 and proteins on hydrophobic polystyrene surfaces studied by neutron reflectometry

Zhenhuan Zhang[a,b], Sara Orski[c], Ann Marie Woys[d], Guangcui Yuan[a,e], Isidro E. Zarraga[d,*], Norman J. Wagner[b,*], Yun Liu[a,b,**]

[a] Center for Neutron Research, National Institute of Standards and Technology, Gaithersburg, MD, 20899, USA
[b] Department of Chemical and Biomolecular Engineering, University of Delaware, Newark, DE, 19716, USA
[c] Polymers and Complex Fluids Group, National Institute of Standards and Technology, Gaithersburg, MD, 29899, USA
[d] Department of Late Stage Pharmaceutical Development, Genentech Inc., San Francisco, CA, 94080, USA
[e] Department of Polymer Engineering, University of Akron, Akron, OH, 44325, USA

ARTICLE INFO

Article history:
Received 9 October 2017
Received in revised form 28 March 2018
Accepted 16 April 2018
Available online 21 April 2018

Keywords:
Polysorbate 20
Monoclonal antibody
Surface adsorption
Neutron reflectometry
Hydrophobic surface

ABSTRACT

Understanding the adsorption of protein and surfactant molecules on hydrophobic surfaces is very important for storage stability and delivery of pharmaceutical liquid formulations as many commonly-used devices, such as drug containers and syringes, have hydrophobic surfaces. Neutron reflectometry is used here to investigate the structure information of the adsorption process of non-ionic surfactant (polysorbate 20) and proteins (monoclonal antibody (mAb) and lysozyme) on polystyrene surfaces. Thickness of adsorbed polysorbate 20 thin film is observed to be ≈21 Å, comparable to the radius of gyration of polysorbate 20 micelles in solution. Although no lysozyme adsorption is observed on the polystyrene surface in low solution pH condition, the mAb can be strongly absorbed on the polystyrene surface with a layer thickness of ≈145 Å. The mAb concentration near the surface is about 135 mg/ml significantly larger than the bulk protein concentration. The differences in adsorption behavior are attributed to different protein interactions with a hydrophobic surface. Further, both surfactants and proteins adsorbed on the polystyrene surfaces can not be rinsed off using pure water.

1. Introduction

Monoclonal antibodies (mAbs) based therapeutic drugs are now the fastest growing section of the pharmaceutical industry due to their excellent target selectivity with fewer side effects compared with traditional small-molecule drugs [1]. To maintain long-term stability of mAbs in solutions, stable buffers containing saccharides, surfactants, and salts, are typically used to provide favorable physio-chemical environment for mAbs, and impede irreversible-aggregate formation during storage and drug administration. Non-ionic surfactant polysorbate 20, also commercially known as Tween^{TM} 20, has been widely used in mAbformulations due to its bio-compatibility, low toxicity, and stabilizing properties.

Despite all the efforts, irreversible aggregations remain a vexing problem for the industry, and may lead to adverse biological consequences [2–4]. Among many possible routes [5–7], irreversible aggregate formation can be initiated through the protein adsorption at solid-liquid and air-liquid interfaces [8]. Therefore, understanding the protein adsorption at different interfaces is important for the pharmaceutical industry to prevent the adsorption from happening. At the same time, the protein adsorption can be also very useful for some other applications since well-controlled protein layers on surfaces can be used as a new generation of reactor beds for biosensor as well as disease diagnostics [9,10]. Because of these interests from both industrial and academic fields, the study of protein adsorption at interfaces has attracted much research attention.

Surface adsorption of proteins and excipients has long been studied on both hydrophilic and hydrophobic surfaces by many methods such as microscopy [11–13], quart crystal microbalance – dissipation (QCM-D) [14,15], ellipsometry [16,17], X-Ray photoelectron spectroscopy (XPS) [13,16], and X-ray/neutron reflectometry [18–21]. Many studies have focused on hydrophobic surfaces, because medical devices, such as infusion tubes or

* Corresponding authors.
** Corresponding author at: Center for Neutron Research, National Institute of Standards and Technology, Gaithersburg, Maryland, 20899, USA.
E-mail addresses: zarraga.isidro@gene.com (I.E. Zarraga), wagnernj@udel.edu (N.J. Wagner), yunliu@udel.edu, yunliu@nist.gov (Y. Liu).

https://doi.org/10.1016/j.colsurfb.2018.04.036
0927-7765/

prefilled syringes, are typically either comprised of hydrophobic polymeric materials or are coated with a layer of hydrophobic oil on glass surfaces to lubricate injection process [22–24]. However, the adsorption behavior of proteins depends on the properties of proteins and surfaces. mAb adsorption on hydrophilic silica surface has been studied with atomic force microscopy (AFM). At relatively low protein concentration, mAb proteins are observed to take predominately a flat-on orientation on the surface [12]. In contrast, a different mAb in solutions with a similar concentration range is believed to take a mixture of orientations including flat-on, side-on, and end-on on 1-docecanethiol surface [15]. A recent study on mAbadsorption in the presence of non-ionic surfactants (polysorbate 20 and polysorbate 80) showed that the amount of protein adsorption depends on the protein and surfactants exposure method on (3, 3-trifluoropropyl) chloromethylsilane surface. In this study, it is observed that the adsorbed protein can only be partially rinsed off by the surfactants [14]. In contrast, a different study showed that complete removal of proteins on the octadecyltrichlorosilane (OTS) surface can be achieved by rinsing the surface with surfactant solutions [11]. The protein adsorption behavior on the OTS surface is found to be sensitive to the relative concentration between proteins and surfactants molecule [11]. The problem is even more complicated when proteins can penetrate the surface. Adsorption of plasma proteins on copolymer hydrogel surfaces have been investigated by measuring thickness changes of hydrogel films with ellipsometry as well as changes in detected surface elements by XPS [17]. The results indicate that absorption of plasma proteins is due to hydrophobic interactions between plasma proteins and copolymer hydrogel. In addition, adsorption is found to be a transport limited process that depends on both the size of proteins and pores formed by hydrophobic sections of the copolymer. Despite many studies of protein adsorption on liquid-solid interfaces, the adsorption mechanism seems still system specific for many cases [8,25].

Amongst the many material choices available for medical devices, polystyrene and polystyrene-coated surfaces, such as STYRON™ 2678 MED, are also used on many devices. However, few studies focus on the adsorption of proteins and excipients on polystyrene surfaces [13,26,27]. Browne et al. studied adsorption of human albumin on polystyrene surfaces using XPS and AFM. They found that human albumin can be irreversibly adsorbed on the surface [13]. Kim et al. studied the adsorption of lysozyme, fibrinogen, and bovine serum albumin on polystyrene surfaces and found that protein structure is more random on hydrophobic polystyrene surfaces compared with that on hydrophilic silica surfaces [28]. In this paper, we investigate adsorption behavior of the non-ionic surfactant, polysorbate 20, and two proteins (mAb-X and lysozyme) by neutron reflectometry on polystyrene surface. Structure of the polysorbate 20 and protein adsorption layer is determined, such as layer thickness, the density distribution, and concentrations near surfaces. Further, we observe large differences in the adsorption behavior of mAb-X compared to lysozyme. While an adsorption layer of mAb-X is observed on the polystyrene surface, lysozyme is not adsorbed on the polystyrene surface at our solution conditions.

2. Materials and methods

2.1. Materials

Pharmacopoeial grade polysorbate 20 (CMC = 8.04×10^{-5} mol/L at 21 °C) [29] and monoclonal antibody mAb-X (pI = 6.75, MW = 150 KDa) were kindly provided by Genentech Inc. Lyophilized lysozyme was purchased from MilliPore(Catalog# 100831), and further purified at CNMS, ORNL following the previous method to remove most salts [30,31]. Polystyrene with molecular weight of 390 KDa ($M_w/M_n < 1.1$ Pressure Chemical Company) was kindly provided by Dr. Kalman Migler from Polymer and Complex Fluids Group at National Institute of Standard and Technology. 99% grade D_2O was purchased from Cambridge Isotope Laboratory. Deionized (DI) water was filtered through 18.2 MΩ before using. Reagent grade Toluene was purchased from J.T. Baker. The substrate made of 3 inches diameter silicon wafers was purchased from Institute of Electronic Material Technology™.

2.2. Preparation of polystyrene surface

Polystyrene was coated on a silicon wafer by spin casting using a solution of 0.5% mass fraction polystyrene in toluene that was mixed with a magnet stirring bar on a hot plate at 120 rpm and 50 °C overnight. The silicon wafer was washed by Micro90 and DI water three times to remove oil from the surface, and then treated in UV/Ozone oven for 1 h to remove any remaining organic contaminants. The wafer was then spin washed by DI water followed by a toluene wash before spin casting polymer solutions. After filtering the solution through a PTFE filter (0.2 μm), the casting solution was slowly dropped onto the surface of a stationary silicon wafer until the wafer surface was fully covered by the solution. The wetted wafer was spin cast at 2500 rmp for 60 s, and then covered by a clean glass petri dish at room temperature for about 30 min. Then the coated wafer with the petri dish was carefully moved into a vacuum oven at 150 °C. Note that the glass transition temperature of polystyrene is between 100 °C and 107 °C [32]. The glass petri dish was used during the annealing process to avoid the contamination of the wafer surface [33]. After annealing the film for 2 h, the sample was cooled down to 25 °C while maintaining a high vacuum of the oven. The coated wafer was subsequently assembled into the NR flow cell [34] and ready for neutron reflectometry measurements. The contact angle of water on the polystyrene coated surface was measured to be approximately 90°, consistent with a previous report [35].

2.3. Sample solutions preparation

1) 20 mM HisOAc buffer with pH = 5.5 preparation: 310.3 mg Histidine and 106 uL Acetic acid were dissolved into 100 mL H_2O and D_2O respectively to make buffers. 2) monoclonal antibody sample preparation: the excipient free monoclonal antibody(mAb-X) was originally provided in liquid state with concentration of 100 mg/ml. To prepare the sample in H_2O, the mAb-X solution was directly diluted into H_2O HisOAc buffer with final concentration of 5 mg/ml. To prepare mAb-X solution in D_2O, 1 mL of mAb-X solution at 100 mg/ml in H_2O buffer was injected into 15 mL (10 K MWCO) centrifugal filter unit and mixed with 14 mL D_2O buffer. The unit was centrifuged at 4000 rpm for 60 min, then it was topped off with D2O buffer. After three iterations, the solution inside the unit was collected and further diluted to 5 mg/ml with D_2O buffer. 3) lysozyme sample preparation: 5 mg/ml of lysozyme sample in D_2O was prepared by reconstituting lyophilized lysozyme powder with D_2O. The resulting solution is at pD = 4.8. 4) polysorbate 20 sample preparation: 1% mass fraction of polysorbate 20 sample was prepared by dissolving 250 mg polysorbate 20 into 25 g D_2O. 50 μL and 520 μL of 1% mass fraction stock solution were pipetted into 10 mL D_2O or H_2O to make solution with a final concentration of 4.075×10^{-5} M (pH = 6.71) and 4.075×10^{-4} M (pH = 6.96) respectively. All solutions were degassed at 635 mm Hg pressure using a TA Degassing Station for 20 min before any measurements.

2.4. Neutron reflectometry measurement and data analysis

Neutron reflectometry measurements were performed at the NG-7 horizontal reflectometer at NIST Center for Neutron Research

(NCNR) with a special liquid flow cell setup that is discussed in literature [34]. By flowing different samples into the flow cell, the same surface can be exposed to different solutions without changing the experiment alignment. First, the polystyrene film in each assembled flow cell was measured by flowing solvent with different contrasts. This was achieved by varying the relative ratio of H_2O and D_2O. By simultaneously analyzing the NR patterns with different contrasts, the coated polystyrene layer on the wafer can be determined accurately [36]. After obtaining the structure of the pure polystyrene film, solutions with either polysorbate 20 or proteins were introduced. The polysorbate 20 and lysozyme solutions were prepared at two contrasts: one set of samples in 100% D_2O (scattering length density (SLD) is 6.3×10^{-6} Å^{-2}) and another set in 100% H_2O (SLD = -0.56×10^{-6} Å^{-2}). NR curves were measured for both sets of samples. To unambiguously obtain the adsorbed mAb-X structure, the mAb-X solution is prepared with solvents at two different D_2O/H_2O ratios(by volume): 100% D_2O, and 88% D_2O/12% H_2O (solvent SLD is 5.5×10^{-6} Å^{-2}, labeled as 5.5 M solvent). For each sample change, measurements were performed after waiting 30 min to allow the system reaching the equilibrium.

NR patterns are analyzed with the DREAM algorithm [37] in Refl1D to simultaneously fit all reflectivity data with different solvent contrasts. During data analysis, the SLD range of Si is constrained between 2.0×10^{-6} Å^{-2} to 2.08×10^{-6} Å^{-2} and SLD of SiO_x is constrained between 3.5×10^{-6} to 4.0×10^{-6} Å^{-2}. Based on previous studies, change in SLD due to water penetration into porous SiO_x layer is allowed [19,20]. The polystyrene film is modeled as a two-layer structure. The inner polymer layer (adjacent to SiO_x) may have a slightly different SLD compared to outer layer due to possible solvent trapping from spin coating or varied packing of the polymer near surface during annealing. The SLD range of the main polystyrene layer is constrained between 1.30×10^{-6} to 1.42×10^{-6} Å^{-2} based on its theoretical value.

From the data fitting, the average SLD profile is obtained as a function of the distance from the Si surface along the normal direction. With the given SLD values, the volume fraction of absorbed sample $\Phi(z)_{sample}$ on the surface can be calculated by

$$\Phi(z)_{sample} = \left(\rho(z)_{before} - \rho(z)_{after}\right) / (\rho_{water} - \rho_{sample}) \quad (1)$$

where $\rho(z)_{before}$ and $\rho(z)_{aftere}$ are SLD profiles before and after the adsorption of sample molecules on the surface. ρ_{water} and ρ_{sample} are SLDs of solvents and samples respectively. SLD of mAb-X is calculated based on amino acid sequence and its partial specific volume(0.74 mL/g) [38,39].

Each adsorption layer on the surface is modeled with a diffuse interface with a Gaussian function. This makes it possible to calculate the composition of each layer starting from the Si surface using an err function as shown in Eq. (2),

$$\Phi = \frac{1}{2}\left[erf\left(\frac{z}{\sqrt{2\sigma_L^2}}\right) - erf\left(\frac{z-d}{\sqrt{2\sigma_R^2}}\right)\right] \quad (2)$$

where d is the thickness of an individual layer, σ_L is root mean square (RMS) surface roughness of the layer with its left neighbor layer, while σ_R is RMS surface roughness of the layer with its right neighbor layer. The sum of volume fraction of each materials on each layer is unit. Therefore, after the composition of each layer is calculated, the volume fraction of water can be obtained by following equation:

$$\Phi(z)_{water} = 1 - \Phi(z)_{Si} - \Phi(z)_{SiOx} - \Phi(z)_{polystyrene} - \Phi(z)_{sample} \quad (3)$$

The total adsorption is estimated by

$$C_{surface} = \frac{\int \Phi_{sample} dz}{d} \times \mu_{sample} \quad (4)$$

where μ_{sample} is the mass density of samples. In this study, mass densities of polysorbate 20 and mAb-X are 1.1 g/cm^3 and 1.35 g/cm^3 respectively according to providers.

Finally, the surface excess can be calculated by [12]

$$\Gamma = C_{surface} \times d \quad (5)$$

2.5. QCM-D measurement

The adsorbed sample mass on a prepared quartz crystal surface can be measured with QCM-D by monitoring its resonant frequency change. Viscoelasticity of absorbed samples layer can be measured by the energy dissipated during the oscillation. An extensive discussion of QCM-D theory and adsorption modeling parameters can be found in the literature [40–42]. Briefly, oscillation of the quartz crystal sensor is generated by applying a radio frequency voltage through gold electrodes on sensors. If the absorbed layer is completely rigid, the absorbed mass of a sample, Δm, can be calculated by the frequency change from its fundamental frequency using Eq. (6).

$$\Delta m = C\frac{\Delta f_z}{z} \quad (6)$$

where C is the Sauerbrey mass sensitivity constant, which is $17.7 ng/cm^2 Hz sf$. And Δf_z is the frequency change on the zth overtone. The viscoelasticity of absorbed samples can be characterized by the dissipation value D as shown in Eq. (7) as

$$D = \frac{1}{\pi f \tau} \quad (7)$$

where τ is the characteristic time scale of the oscillation's exponential decay, and f is the resonant frequency. In general, if D is on the order of 10^{-6}, the absorbed film can be considered viscoelastic.

To prepare our samples for the QCM-D experiments, polystyrene solution was spin coated on crystal sensors following the same protocol as described for NR experiments. Coated sensors were installed into the flow cell first to allow for oscillation in air until the oscillation equilibrium was reached. H_2O was then injected into the flow cell by a peristaltic pump at 50 μL/min for approximately 1000 s until the baseline of the QCM-D was stable. Sample solutions (with the concentrations at 4.075×10^{-5} M and 4.075×10^{-4} M polysorbate 20) were introduced into the cell with a flow rate at 50 μL/min until the frequency and dissipation signals no longer change. Then, the sample cell was rinsed with pure H_2O until signals. To determine if additional polysorbate could be adsorbed after exposure to higher concentration PS20, 4.075×10^{-4} M PS20 solution was introduced after the sensor was first exposed to 4.075×10^{-5} M polysorbate 20. The Sauerbrey function is used to model the signal change to extract the adsorbed mass of surfactants on the sensor surface.

3. Results and discussions

3.1. Adsorption of polysorbate20 on the polystyrene surface

NR data for a bare polystyrene film exposed to 100% D_2O (gray squares) and 100% H_2O (gray triangles) are shown in Fig. 1a. The blue solid and dash lines in Fig. 1a are the fitting results by simultaneously analyzing these two NR curves. From the fitting results, the thickness of the polystyrene film is observed to be ≈225 Å, which agrees with the literature value [43].

NR patterns after introducing polysorbate 20 solution into the flow cell are shown in Fig. 1b. As shown in the supporting information (Fig. S-1), the NR fringe spacing shows clear shifts after polysorbate 20 is injected into the flow cell, indicating the adsorption of polysorbate 20 onto the polystyrene surface. This observation is not surprising as polysorbate 20 has a bulky

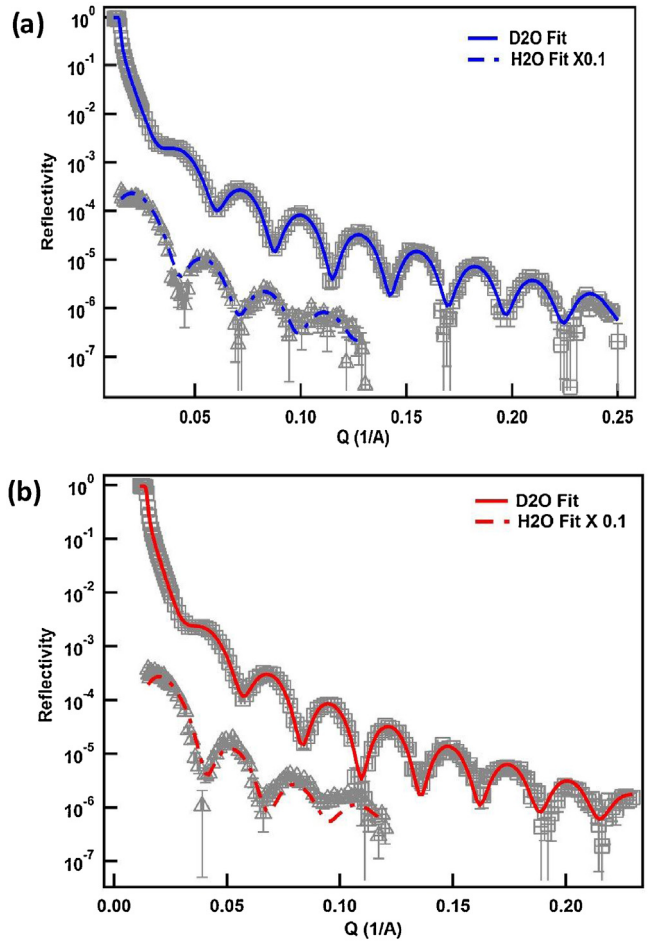

Fig. 1. Neutron reflectivity measurement results. (a): raw reflectivity data of polystyrene film measured in D_2O (grey square), H_2O X 0.1 (grey triangle), and fitting results of D_2O (blue solid line), H_2O X 0.1 (blue dot line). (b): raw reflectivity data of polysorbate 20 solution with concentration of 4.075×10^{-4} M absorbed on polystyrene film in D_2O (grey square), H_2O X 0.1 (grey cross), and fitting results of D_2O (red solid line), H_2O X 0.1 (red dot line). (For interpretation of the references to colour in this figure legend, the reader is referred to the web version of this article.)

hydrophilic polyoxyethylene head connected with a hydrophobic fatty acid tails [44,45]. Due to its amphiphilic nature, polysorbate 20 is expected to be adsorbed to hydrophobic surfaces. From the fitting results, the quantitative structural information of the adsorbed polysorbate 20 can be extracted. The fitting results (the red lines) agree well with the experimental results. The results of all fitting parameters are shown in Table 1 in supporting information.

The obtained SLD profile, starting from the silicon surface, is shown in Fig. 2. Compared to the SLD profile of pure polystyrene film with D_2O, there is a clear drop in the SLD near the polystyrene surface after polysorbate 20 is introduced into the flow cell. This indicates the replacement of D_2O (SLD = 6.33×10^{-6} Å^{-2}) molecules by polysorbate 20 (SLD = 0.8×10^{-6} Å^{-2}) at the interface. The black line (Fig. 2) shows the change of two SLD profiles before and after the polysorbate 20 is added. Thus, the black line represents the SLD profile of only adsorbed polysorbate 20 at the polystyrene surface. Thickness of this adsorbed layer is about 21 Å, which is comparable to the radius of gyration of polysorbate 20 [46,47]. Due to the maximum Q achievable with the NR instrument ($\pi/Q_{max} \approx 15$ Å with two contrasts), our results are not sensitive enough to the detailed shape of the polysorbate layer even though it is very sensitive to the layer thickness. The adsorption of polysorbate 20, 40, 60, and 80 on an octadecyltriethoxysilane surface was also studied by the ellipsometry [16]. It was shown that the adsorbed layer thickness of polysorbate 20 is about 19 Å, consistent with the adsorption behavior on the polystyrene surface studied here.

The volume fraction of different materials in each layer is estimated using the obtained SLD information and shown in Fig. 3. The average volume fraction of polysorbate 20 at the surface layer is about 51%, which is estimated by averaging over the entire adsorption layer for polysorbate 20. The volume fraction may be further converted to the mass concentration (550 mg/ml), which is ~1100 times higher than the bulk polysorbate 20 concentration used here. Hence, a highly concentrated polysorbate 20 layer forms on the polystyrene surface. Due to the bulky hydrophilic head of polysorbate 20, the adsorbed layer should be highly hydrated. Therefore, a volume fraction of 51% may suggest a monolayer coverage. However, as the surface roughness could change the surface morphology of adsorbed surfactants, the exact structures of polysorbate 20 on a hydrophobic surface needs further studies. The measured surface excess of polysorbate 20 is around 1.16 mg/m^2, from which the estimated area per molecule is 175 Å^2 on the surface.

To check if adsorbed surfactant molecules can be easily desorbed, pure water was flowed over the PS20-adsorbed surface. Interestingly, the NR curves show no change at all after flowing pure water through the flow cell for a few hours, indicating that once the surfactant molecules are adsorbed on this hydrophobic surface, they cannot be easily rinsed off within the experiment time scale (8 h) as shown in Fig. S-2 in supporting information.

Surface adsorption of polysorbate 20 can be also measured with QCM-D. The time resolution of QCM-D allows us to retrieve the information of adsorption kinetics. Fig. 4 shows the change of resonant frequency and dissipation parameter as a function of time after the polysorbate 20 is introduced into the cell. Adsorption occurs very rapidly. Frequency and dissipation of the QCM-D stabilize after ~500 s. For all experiments, the dissipation contribution is relatively small with the dissipation value, D, less than 2×10^{-6}. The Sauerbrey model is used in lieu of more complex viscoelastic models for this study. Resulting hydrated masses of absorbed polysorbate 20 are 2.27 ± 0.21 mg/m^2 and 2.45 ± 0.11 mg/m^2 for bulk concentrations of 4.075×10^{-5} M and 4.075×10^{-4} M respectively (the surface excess measured by QCM-D is the hydrated mass, which is expercted to be higher than the result from NR). Our results indicate that polysorbate 20 adsorption is not very sensitive to bulk solution concentrations, which agrees with NR data (Fig. S-3 in supporting information). NR curves for different concentrations are identical.

3.2. Adsorption of mAb-X on polystyrene surface

Compared to polysorbate 20, the radius of gyration of mAb-X in solution is ≈ 5 nm much larger than that of polysorbate 20 [48]. Similar to polysorbate 20, comparison of the NR data before and after the adsorption of proteins shows an obvious change after mAb-X solution is infused into the flow cell (as shown in supporting information S-4). This clearly indicates that mAb-X is adsorbed on the polystyrene surface. The best fitting of absorbed mAb-X is modeled by two layers. And water is permitted to diffuse into each layer in our model. Any hydrogen-deuterium exchange of labile hydrogens in the protein is considered in the fitting, which leads to higher protein SLD in D_2O compared to H_2O [49]. As mentioned, to unambiguously extract the structure of adsorbed mAb-X, solvent contrast is varied by changing the D_2O/H_2O ratio. The data is simultaneously fitted with results from two solvent contrasts as shown in Fig. 5. The results with only buffer in the flow cell are shown in Fig. 5a and the result with 5 mg/ml mAb-X solution are shown in Fig. 5b. The agreement is excellent between the fitting curves (lines) and the experimental data (symbols).

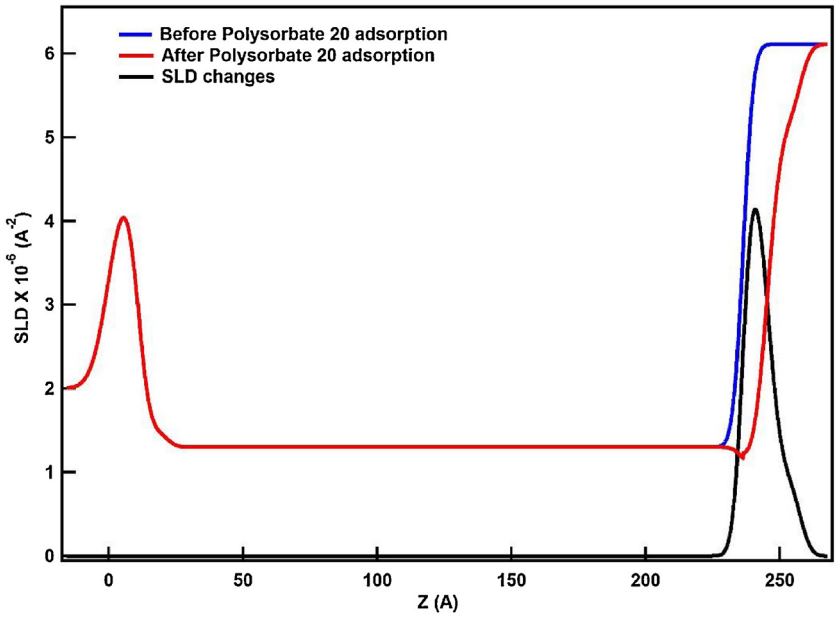

Fig. 2. Scattering length density (SLD) profile in D_2O before (blue line) and after (red line) 4.075×10^{-4} M polysorbate 20 adsorption on polystyrene film. Changes in the SLD profile after 4.075×10^{-4} M polysorbate 20 adsorption is plotted as the black line. (For interpretation of the references to colour in this figure legend, the reader is referred to the web version of this article.)

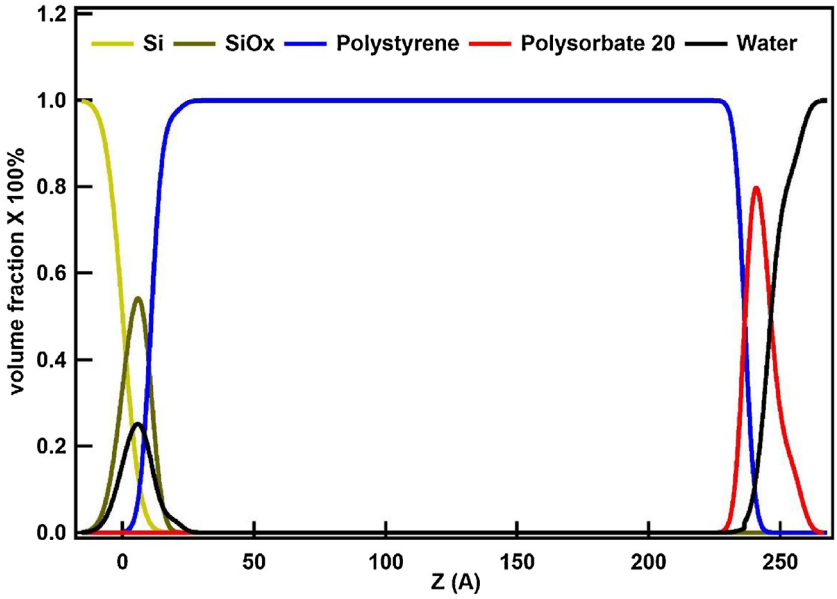

Fig. 3. Volume fractions of each layers after 4.075×10^{-4} M polysorbate 20 adsorption on polystyrene surface: silicon (gold), SiO_x (brown), polystyrene (blue), polysorbate 20 (red), water (black). (For interpretation of the references to colour in this figure legend, the reader is referred to the web version of this article.)

SLD profiles of polystyrene coated wafer before and after flowing the protein solution through the flow cell are obtained from the best fitting results and shown in Fig. 6. The SLD change before and after the mAb-X absorption is characterized by two regions (black line, Fig-6). The layer close to the polystyrene surface is about 66 Å thick, while the outer layer is about 79 Å thick. The volume fraction of mAb-X in the inner layer is about 14% which is exactly two times of that of the outer layer (7%). The distribution of the volume fraction suggested an end-on (Fab-down) orientation of the protein molecule on the surface as shown in Fig. 7b. To find the surface concentration of absorbed mAb-X, mAb-X volume fraction is calculated from Eq. (1). The results are plotted in Fig. 7a. The volume fraction of mAb-X after averaging both the inner and outer layers is about 10%. This corresponds to mAb-X concentration of 135 mg/ml near the polystyrene surface. All fitting parameters are provided in Table 2 in supporting information. The surface excess of absorbed mAb-X is estimated from Eq. (5) and is about 1.97 mg/m^2. The average area per protein in the absorbed layer is around 13000 Å^2. It is noted that the study by Buijs et al., showed that the surface excess of investigated mAbs can range from 3.7 to 5.5 mg/m^2 on the charged hydrophobic polymeric surfaces, which is larger than what we have [50].

3.3. Adsorption of lysozyme on polystyrene surface

Lysozyme molecule is significantly smaller than mAbs. The radius of gyration is only about 1.4 nm [51]. It is well known that lysozyme can form dense layers on air-water and solid-liquid interfaces [52–55]. Because lysozyme has both hydrophilic and hydrophobic patches on its surface, it can be adsorbed to

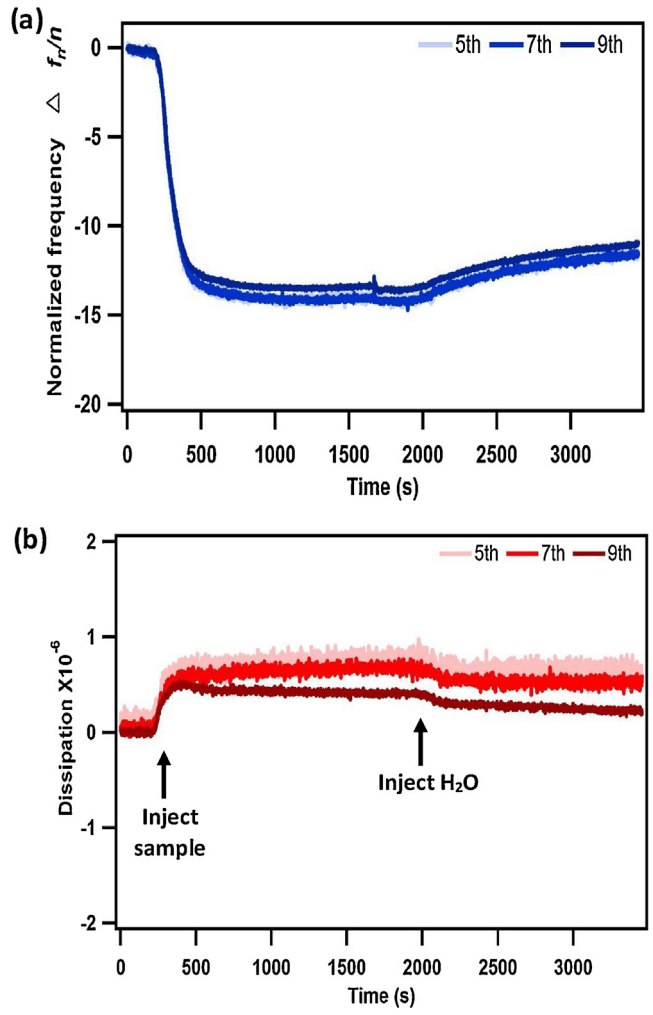

Fig. 4. (a): normalized frequency changes of each overtone after 4.075×10^{-5} M polysorbate 20 is infused into flow cell and (b): corresponding dissipation value of each overtone.

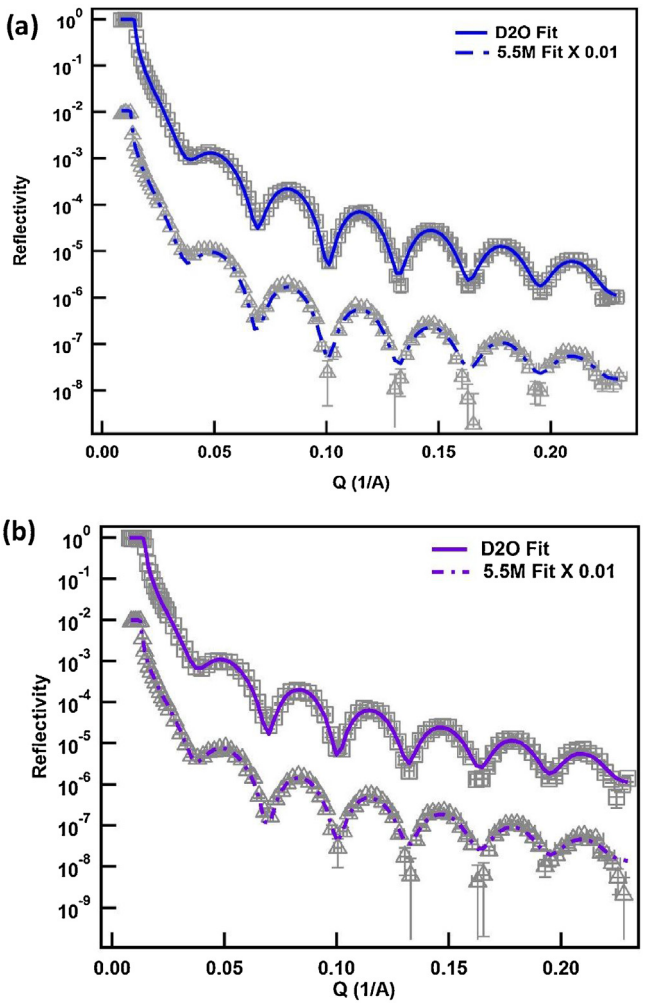

Fig. 5. Neutron reflectivity measurement results. (a): Raw reflectivity data of polystyrene film measured in D_2O (grey square), 5.5-match water x0.01 (grey triangle), and fitting results of D_2O (blue solid line), 5.5-match water x0.01 (blue dash-dot line). (b): raw reflectivity data of mAb-X solution with concentration of 5 mg/ml absorbed on polystyrene film D_2O (purple solid line), 5.5-match water x0.01 (purple dash-dot line). (For interpretation of the references to colour in this figure legend, the reader is referred to the web version of this article.)

hydrophilic surfaces through electrostatic attractions as well as to hydrophobic surfaces by hydrophobic interactions. Both interactions may induce unfolding of secondary structure and thereby lead to loss of its globular shape [54]. Therefore, it is possible that lysozyme could partially unfold and be adsorbed to the hydrophobic polystyrene surface. However, our reflectivity pattern does not change after 5 mg/ml lysozyme is exposed to the polystyrene surface as shown in Fig. 8. Thus, lysozyme cannot be absorbed onto the polystyrene surface in this case. To explain this observation, we hypothesize that the image charge effects introduces a repulsion to charged lysozyme so that lysozyme protein cannot access the solid interface [56]. In addition, the commercial lysozyme was further purified to remove most salts before lyophilization for our experiments [30,31]. Ionic strength of the lysozyme solution should be very low. As its pI is 11.35, lysozyme carries large amount of positive charges on its surface in the solution(Concentration = 5 mg/ml, pD = 4.8) [57]. When lysozyme approaches a polystyrene surface, a positive image charges may form in polystyrene layer due to the significant difference of dielectric constant between water ($\varepsilon_w = 78$) and polystyrene ($\varepsilon_p = 3$). The image charges can be calculated by Eq. (8) as [56,58]:

$$q_{image} = q_{lysozyme} \frac{\varepsilon_w - \varepsilon_p}{\varepsilon_w + \varepsilon_p} \quad (8)$$

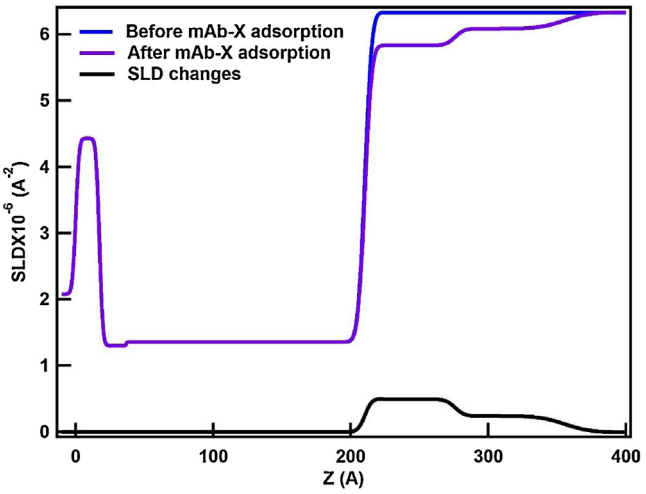

Fig. 6. Scattering length density(SLD) profile in D_2O before 5 mg/ml mAb-X adsorption on polystyrene film (blue line) and after 5 mg/ml mAb-X adsorption on polystyrene film (purple line). Changes in the SLD profile after 5 mg/ml mAb-X adsorption is plotted as the black line. (For interpretation of the references to colour in this figure legend, the reader is referred to the web version of this article.)

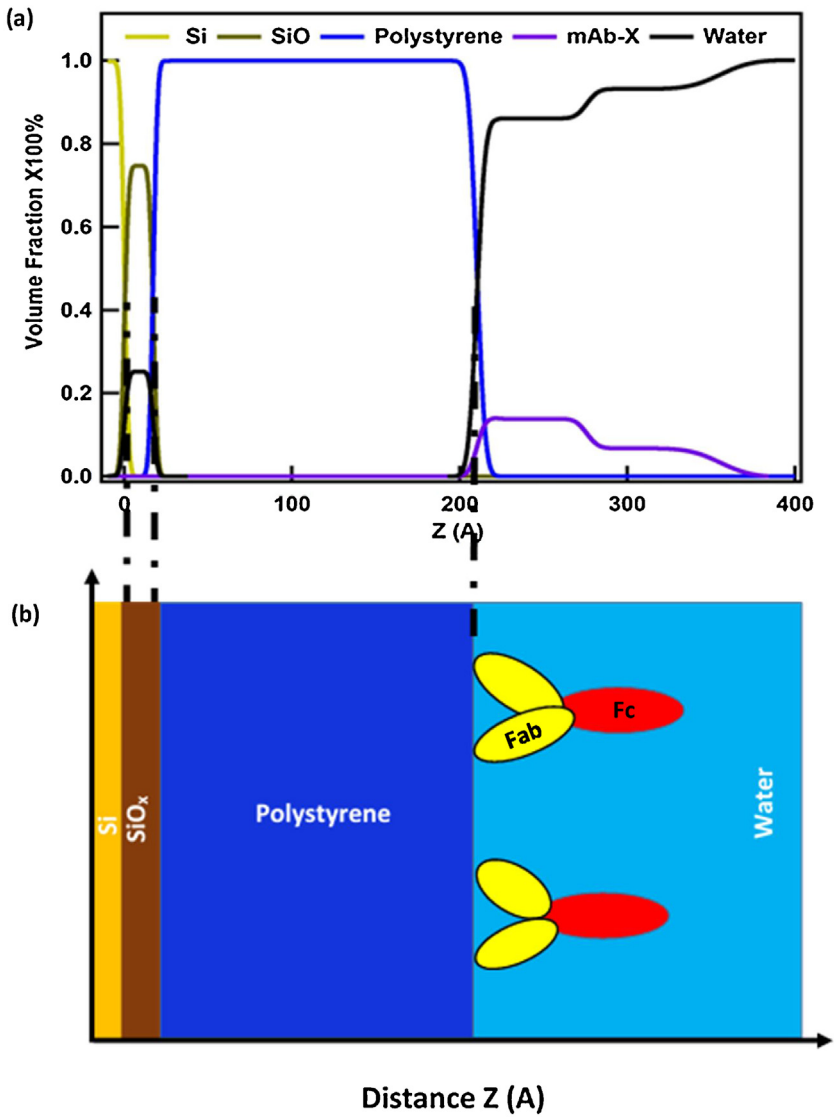

Fig. 7. (a): Volume fractions of each layers after 5 mg/ml mAb-X adsorption on polystyrene surface: silicon (gold), SiO_x (brown), polystyrene (blue), mAb-X (purple), water (black). (b): possible mAb-X surface morphology after adsorption. (For interpretation of the references to colour in this figure legend, the reader is referred to the web version of this article.)

It has been shown that the repulsion force generated from this image charge effect can be dominant among others such as van der Waals force and electric double layer force [58]. Therefore, the adsorption of lysozyme can be prevented under this physiochemical condition. We also measured NR data for lysozyme solutions at higher concentration such as 25 mg/ml, 50 mg/ml, 75 mg/ml (Data are not shown here.) However, surprisingly, there is no adsorption observed based on our neutron reflectometry measurements. Lysozyme adsorption has been observed on some hydrophobic surfaces, such as octadecyltrichlorosilane (OTS) surface [54]. It is noted that in Ref. [54] lysozyme solutions at similar pH values is also studied and the surface adsorption is observed by the NR. Comparing our experiment to the experiment in Ref. [54], we note a few differences here. First, the polystyrene surface is used in this paper instead of OTS. Secondly, the polymer film thickness is about 225 Å instead of much thinner layer about 26 Å. Thirdly, lysozyme used in this paper has been further purified after they were purchased. At present, it is still not clear to us which one is the dominating factor that causes the different experimental observations, which need a future study on this topic.

4. Conclusion

Quantitative understanding of proteins and excipients adsorption to hydrophobic surfaces is relevant for many practical challenges in pharmaceutical industries. In this work, the adsorption of non-ionic surfactant polysorbate 20, mAb-X protein, and lysozyme protein on polystyrene surface are investigated using neutron reflectometry. Not surprisingly, when the hydrophobic polystyrene surface is exposed to polysorbate 20 solutions, a dense film of polysorbate 20 forms at the surface. Thickness of absorbed polysorbate 20 layer is 21 Å, which is comparable to the radius of polysorbate 20 micelles. Adsorption of surfactant is irreversible and not sensitive to bulk concentration. Moreover, from QCM-D measurements of polysorbate 20, adsorption kinetics are fast after the polysorbate 20 solutions are introduced to a polystyrene surface. The adsorption behaviors of mAb-X and lysozyme proteins are also investigated by the neutron reflectometry method. The two proteins behave differently. For mAb-X molecules, we observe a single adsorption layer with an end-on (Fab-down) orientation on the polystyrene surface. In contrast, lysozyme does not adsorb to

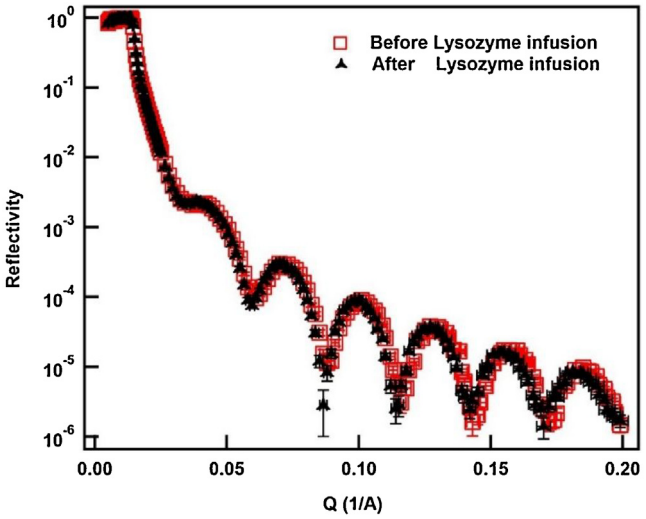

Fig. 8. reflectivity data of polystyrene film in D_2O (red square), and after 5 mg/ml lysozyme solution is infused into flow cell (black triangle). (For interpretation of the references to colour in this figure legend, the reader is referred to the web version of this article.)

the polystyrene surface at the investigated concentrations at our experimental conditions. We speculate that this is mainly due to the image charge effects. The quantitative, molecular-scale data obtained herein will be useful for theorists and simulators modeling adsorption and provides a method and basis for competitive adsorption studies in future.

Acknowledgements

The authors thank Dr. Kalman Migler for providing the polystyrene used in this study, and useful discussions with Dr. Bulent Akgun, Dr. Frank Heinrich, Dr. Sushil K. Satija, and Dr. David Hoogerheide. Certain commercial equipment, instruments, or materials (or suppliers, or software, ...) are identified in this paper to foster understanding. Such identification does not imply recommendation or endorsement by the National Institute of Standards and Technology, nor does it imply that the materials or equipment identified are necessarily the best available for the purpose. This manuscript was prepared under the partial support of the cooperative agreements 70NANB15H260 and 70NANB10H256 from NIST, U.S. Department of Commerce.

Appendix A. Supplementary data

Supplementary data associated with this article can be found, in the online version, at https://doi.org/10.1016/j.colsurfb.2018.04.036.

References

[1] S.J. Shire, 1 – Introduction, Monoclonal Antibodies, Woodhead Publishing, 2015, pp. 1–15.
[2] J.A. Hubbell, Biomaterials in tissue engineering, Nat. Biotechnol. 13 (1995) 565–576.
[3] C. Sandu, R. Singh, Energy increase in operation and cleaning due to heat-exchanger fouling in milk pasteurization, Food Technol 32 (84–91) (1991) 3.
[4] C.J. Roberts, Protein aggregation and its impact on product quality, Curr. Opin. Biotechnol. 30 (2014) 211–217.
[5] S. Amin, G.V. Barnett, J.A. Pathak, C.J. Roberts, P.S. Sarangapani, Protein aggregation particle formation, characterization & rheology, Curr. Opini. Colloid Interface Sci. 19 (2014) 438–449.
[6] E.Y. Chi, S. Krishnan, T.W. Randolph, J.F. Carpenter, Physical stability of proteins in aqueous solution: mechanism and driving forces in nonnative protein aggregation, Pharm. Res. 20 (2003) 1325–1336.
[7] H.J. Lee, A. McAuley, K.F. Schilke, J. McGuire, Molecular origins of surfactant-mediated stabilization of protein drugs, Adv. Drug Deliv. Rev. 63 (2011) 1160–1171.
[8] C. Pinholt, R.A. Hartvig, N.J. Medlicott, L. Jorgensen, The importance of interfaces in protein drug delivery –why is protein adsorption of interest in pharmaceutical formulations? Expert Opin. Drug Deliv. 8 (2011) 949–964.
[9] W. Inglis, G.H. Sanders, P.M. Williams, M.C. Davies, C.J. Roberts, S.J. Tendler, A simple method for biocompatible polymer based spatially controlled adsorption of blood plasma proteins to a surface, Langmuir 17 (2001) 7402–7405.
[10] B.D. Martin, B.P. Gaber, C.H. Patterson, D.C. Turner, Direct protein microarray fabrication using a hydrogel stamper, Langmuir 14 (1998) 3971–3975.
[11] R.G. Couston, M.W. Skoda, S. Uddin, C.F. van der Walle, Adsorption Behavior of a Human Monoclonal Antibody at Hydrophilic and Hydrophobic Surfaces, Mabs Taylor & Francis, 2013, pp. 126–139.
[12] H. Xu, X. Zhao, C. Grant, J.R. Lu, D.E. Williams, J. Penfold, Orientation of a monoclonal antibody adsorbed at the solid/solution interface: a combined study using atomic force microscopy and neutron reflectivity, Langmuir 22 (2006) 6313–6320.
[13] M. Browne, G. Lubarsky, M. Davidson, R. Bradley, Protein adsorption onto polystyrene surfaces studied by XPS and AFM, Surf. Sci. 553 (2004) 155–167.
[14] S.J. Kapp, I. Larsson, M.V. De Weert, M. Cárdenas, L. Jorgensen, Competitive adsorption of monoclonal antibodies and nonionic surfactants at solid hydrophobic surfaces, J. Pharm. Sci. 104 (2015) 593–601.
[15] M.E. Wiseman, C.W. Frank, Antibody adsorption and orientation on hydrophobic surfaces, Langmuir 28 (2012) 1765–1774.
[16] M. Graca, J.H. Bongaerts, J.R. Stokes, S. Granick, Friction and adsorption of aqueous polyoxyethylene (Tween) surfactants at hydrophobic surfaces, J. Colloid Interface Sci. 315 (2007) 662–670.
[17] G. Guzman, S.M. Bhaway, T. Nugay, B.D. Vogt, M. Cakmak, Transport-limited adsorption of plasma proteins on bimodal amphiphilic polymer co-networks: real-lime studies by spectroscopic ellipsometry, Langmuir 33 (2017) 2900–2910.
[18] S.S. Pai, F. Heinrich, A.L. Canady, T.M. Przybycien, R.D. Tilton, Coverage-dependent morphology of PEGylated lysozyme layers adsorbed on silica, J. Colloid Interface Sci. 370 (2012) 170–175.
[19] E. Schneck, I. Berts, A. Halperin, J. Daillant, G. Fragneto, Neutron reflectometry from poly (ethylene-glycol) brushes binding anti-PEG antibodies: evidence of ternary adsorption, Biomaterials 46 (2015) 95–104.
[20] E. Schneck, A. Schollier, A. Halperin, M. Moulin, M. Haertlein, M. Sferrazza, G. Fragneto, Neutron reflectometry elucidates density profiles of deuterated proteins adsorbed onto surfaces displaying poly (ethylene glycol) brushes: evidence for primary adsorption, Langmuir 29 (2013) 14178–14187.
[21] Z. Li, R. Li, C. Smith, F. Pan, M. Campana, J.R.P. Webster, C.F. van der Walle, S. Uddin, S.M. Bishop, R. Narwal, J. Warwicker, J.R. Lu, Neutron reflection study of surface adsorption of fc, fab, and the whole mAb, ACS Appl. Mater. Interfaces 9 (2017) 23202–23211.
[22] E. Chan, A. Hubbard, S. Sane, Y.-F. Maa, Syringe siliconization process investigation and optimization, PDA J. Pharm. Sci. Technol. 66 (2012) 136–150.
[23] A. Gerhardt, A.C. Mcumber, B.H. Nguyen, R. Lewus, D.K. Schwartz, J.F. Carpenter, T.W. Randolph, Surfactant effects on particle generation in antibody formulations in pre-filled syringes, J. Pharm. Sci. 104 (2015) 4056–4064.
[24] M. Reinhard, R. Bouffleur, M. Spallek, Method of producing a filled plastic syringe body for medical purposes, Google Patents, 2000.
[25] V. Hlady, J. Buijs, Protein adsorption on solid surfaces, Curr. Opin. Biotechnol. 7 (1996) 72–77.
[26] S. Koutsopoulos, K. Patzsch, W.T.E. Bosker, W. Norde, Adsorption of trypsin on hydrophilic and hydrophobic surfaces, Langmuir 23 (2007) 2000–2006.
[27] D. Lazos, S. Franzka, M. Ulbricht, Size-Selective protein adsorption to polystyrene surfaces by self-assembled grafted poly(ethylene glycols) with varied chain lengths, Langmuir 21 (2005) 8774–8784.
[28] J. Kim, G.A. Somorjai, Molecular packing of lysozyme, fibrinogen, and bovine serum albumin on hydrophilic and hydrophobic surfaces studied by infrared-Visible sum frequency generation and fluorescence microscopy, J. Am. Chem. Soc. 125 (2003) 3150–3158.
[29] C. Kim, Y.-L. Hsieh, Wetting and absorbency of nonionic surfactant solutions on cotton fabrics, Coll. Surf. A 187–188 (2001) 385–397.
[30] P.D. Godfrin, S.D. Hudson, K. Hong, L. Porcar, P. Falus, N.J. Wagner, Y. Liu, Short-Time glassy dynamics in viscous protein solutions with competing interactions, Phys. Rev. Lett. 115 (2015) 228302.
[31] J. Riest, G. Nägele, Y. Liu, N.J. Wagner, P.D. Godfrin, Short-time dynamics of lysozyme solutions with competing short-range attraction and long-range repulsion: experiment and theory, J. Chem. Phys. 148 (2018) 065101.
[32] J. Rieger, The glass transition temperature of polystyrene, J. Therm. Anal. 46 (1996) 965–972.
[33] Y.-S. Seo, S. Satija, No intrinsic depletion layer on a polystyrene thin film at a water interface, Langmuir 22 (2006) 7113–7116.
[34] J. Fitter, T. Gutberlet, J. Katsaras, Neutron Scattering in Biology: Techniques and Applications, Springer Science & Business Media, 2006.
[35] Y. Li, J.Q. Pham, K.P. Johnston, P.F. Green, Contact angle of water on polystyrene thin Films: effects of CO2 environment and film thickness, Langmuir 23 (2007) 9785–9793.
[36] J. Liepe, S. Filippi, M. Komorowski, M.P. Stumpf, Maximizing the information content of experiments in systems biology, PLoS Comput. Biol. 9 (2013) e1002888.

[37] J.A. Vrugt, C.J. Ter Braak, H.V. Gupta, B.A. Robinson, Equifinality of formal (DREAM) and informal (GLUE) Bayesian approaches in hydrologic modeling? Stoch. Environ. Res. Risk Assess. 23 (2009) 1011–1026.
[38] H. Zhao, P.H. Brown, P. Schuck, On the distribution of protein refractive index increments, Biophys. J. 100 (2011) 2309–2317.
[39] P.H. Brown, A. Balbo, H. Zhao, C. Ebel, P. Schuck, Density contrast sedimentation velocity for the determination of protein partial-specific volumes, PLoS One 6 (2011) e26221.
[40] I. Reviakine, D. Johannsmann, R.P. Richter, Hearing What You Cannot See and Visualizing What You Hear: Interpreting Quartz Crystal Microbalance Data from Solvated Interfaces, ACS Publications, 2011.
[41] B.D. Vogt, E.K. Lin, W.-l. Wu, C.C. White, Effect of film thickness on the validity of the Sauerbrey equation for hydrated polyelectrolyte films, J. Phys. Chem. B 108 (2004) 12685–12690.
[42] N.B. Eisele, F.I. Andersson, S. Frey, R.P. Richter, Viscoelasticity of thin biomolecular films: a case study on nucleoporin phenylalanine-glycine repeats grafted to a histidine-tag capturing QCM-D sensor, Biomacromolecules 13 (2012) 2322–2332.
[43] D.B. Hall, P. Underhill, J.M. Torkelson, Spin coating of thin and ultrathin polymer films, Polym. Eng. Sci. 38 (1998) 2039–2045.
[44] F. Ayorinde, S.V. Gelain, J. Johnson, L.W. Wan, Analysis of some commercial polysorbate formulations using matrix-assisted laser desorption/ionization time-of-flight mass spectrometry, Rapid Commun. Mass Spectrom. 14 (2000) 2116–2124.
[45] M. Lapelosa, T.W. Patapoff, I.E. Zarraga, Molecular simulations of micellar aggregation of polysorbate 20 ester fractions and their interaction with N-phenyl-1-naphthylamine dye, Biophys. Chem. 213 (2016) 17–24.
[46] J. Nayem et al. Studying Morphology and Thermal Stability of Individual and Mixed Components of Polysorbate 20 and 80 via Small Angle Neutron Scattering, To be submitted.
[47] M. Lapelosa, T.W. Patapoff, I.E. Zarraga, Molecular simulations of micellar aggregation of polysorbate 20 ester fractions and their interaction with N-phenyl-1-naphthylamine dye, Biophys. Chem. 213 (2016) 17–24.
[48] E.J. Yearley, P.D. Godfrin, T. Perevozchikova, H. Zhang, P. Falus, L. Porcar, M. Nagao, J.E. Curtis, P. Gawande, R. Taing, Observation of small cluster formation in concentrated monoclonal antibody solutions and its implications to solution viscosity, Biophys. J. 106 (2014) 1763–1770.
[49] A.R. Mazzer, L.A. Clifton, T. Perevozchikova, P.D. Butler, C.J. Roberts, D.G. Bracewell, Neutron reflectivity measurement of protein A—antibody complex at the solid-liquid interface, J. Chromatogr. A 1499 (May) (2017) 118–131.
[50] J. Buijs, J.W.T. Lichtenbelt, W. Norde, J. Lyklema, Adsorption of monoclonal IgGs and their F(ab′)2 fragments onto polymeric surfaces, Colloids Surf. B: Biointerfaces 5 (1995) 11–23.
[51] W.R. Krigbaum, F. Kügler, Molecular conformation of egg-white lysozyme and bovine (-lactalbumin in solution, Biochemistry 9 (1970) 1216–1223.
[52] S.M. Daly, T.M. Przybycien, R.D. Tilton, Coverage-dependent orientation of lysozyme adsorbed on silica, Langmuir 19 (2003) 3848–3857.
[53] J.R. Hunter, P.K. Kilpatrick, R.G. Carbonell, Lysozyme adsorption at the air/water interface, J. Colloid Interface Sci. 137 (1990) 462–482.
[54] J.R. Lu, T.J. Su, P.N. Thirtle, R.K. Thomas, A.R. Rennie, R. Cubitt, The denaturation of lysozyme layers adsorbed at the hydrophobic solid/liquid surface studied by neutron reflection, J. Colloid Interface Sci. 206 (1998) 212–223.
[55] G. Raffaini, F. Ganazzoli, Protein adsorption on a hydrophobic surface: a molecular dynamics study of lysozyme on graphite, Langmuir 26 (2010) 5679–5689.
[56] J.N. Israelachvili, Intermolecular and Surface Forces, Academic press, 2011.
[57] D.E. Kuehner, J. Engmann, F. Fergg, M. Wernick, H.W. Blanch, J.M. Prausnitz, Lysozyme net charge and ion binding in concentrated aqueous electrolyte solutions, J. Phys. Chem. B 103 (1999) 1368–1374.
[58] H. Wang, V. Singh, S.H. Behrens, Image charge effects on the formation of pickering emulsions, J. Phys. Chem. Lett. 3 (2012) 2986–2990.